FINITE ELEMENT ANALYSIS OF PIPE WHIP RESTRAINTS SI3R-640A, FWR-35 AND FWR-16

Commonwealth Edison Company
Byron and Braidwood Stations - Units 1 and 2
Project Nos. 4391/4392 and 4683/4684

J. Pop, Jr.
M. S. Yang
M. Amin

Nuclear Safety-Related

Revision 0 - September 1984

SARGENT & LUNDY ENGINEERS

Report No.
SAD-442

Structural Analytical Division

Report Issue Summary

Project I.D.	Project Name	Byron/Braidwood	Number	4391/4392 4683/4684
	Client	Commonwealth Edison Company		
Document I.D.	Report Title	Finite Element Analysis of Pipe Whip Restraints SI3R-640A, FWR-35 and FWR-16		
	Report Number	SAD-442	Nuclear Safety Related	Yes [XX] No [ ]

Revision No. & Date	Signatures	Date	Identification of Revised Pages
Revision 0	Prepared by: John Pop Jr.	9-12-84	
	[illegible]	9-12-84	
	Reviewed by: [illegible]	9-12-84	
	Approved by: [illegible]	9-12-84	

TABLE OF CONTENTS

I. SUMMARY

In discussions of the test plan for qualification of energy absorbing material (EAM) with NRC Region III and NRR Staff, CECo was requested to provide the design drawings for all Byron/Braidwood pipe whip restraints that use EAM (Reference 1). The staff was to review the drawings to determine whether the load angularities considered in the EAM test plan bound all design conditions. As a result of this review, the staff indicated in a letter dated July 21, 1983, that the design of FWR-35 and SI3R-640A restrains is not bounded by the EAM test for the following reasons:

"The staff believes that the tension member for two restrains (identified as FWR-35 nd SI3R-640A) will be in compression (not tension) during the initial loading phase. Consequently, the EAM will be subjected to a load angularity and deformation not explicity considered in the restraint design nor in the test plan. Furthermore, the EAM will be subjected to an additional bending moment (in conjunction with the compressive and lateral loadings) which is also not considered in the restraint design nor in the test plan."

In order to address the concerns stated above, CECo proposed to perform a detailed finite element analysis of the two restraints. This report summarizes the detailed nonlinear finite element analysis performed on these two pipe whip restraints (SI3R-640A and FWR-35).

Subsequent to the analysis of FWR-35 locations on the feedwater system were reviewed and revised. As a result of this review, FWR-35 was deleted. Because of this deletion, another two-legged restraint, FWR-16, was added to the study scope of the behavior of two-legged restraints. This addition was prompted by the fact that in SI3R-640A and FWR-35 the angle between the pipe break direction and the tension leg is less than 90° in each case. In FWR-16 this angle is 91° being closest to the range of angle which has been of interest to NRC Staff. Subsequent to its selection, restraint FWR-16 was also deleted.

In this report the details of modeling, method of analysis and results of the analysis are presented for the restraint SI3R-640A. Only the results of the analysis for the deleted restraint FWR-35 and FWR-16 are presented in Appendix A and B respectively. The analysis presented herein shows that these restraints can withstand the postulated pipe break force without exceeding strain limits in the tension rod and energy-absorbing material. Therefore, they will satisfactorily perform their intended function.

II. RESTRAINT DESCRIPTION

SI3R-640A is a two-legged restraint located on loop 4 of the safety injection system. Figure 1 shows the locations of the restraint and of the three circumferential pipe breaks affecting the restraint on the 10-inch O.D. line. The restraint is designed to transmit the postulated pipe break forces through the steel box girders to the embedment plates on the containment wall and secondary shield wall. The restraint construction is shown in Figure 2. Tension forces are transmitted through two tension (7/8" Ø A193-B7) rods. Compression force is transmitted through a honeycomb material (5" x 4" x 3" thick) and a W8x35 structural steel. The direction of break forces on the restraint, is shown in Figure 2. The effective gap between the pipe and the restraint is 1.754 inches.

III. METHOD OF ANALYSIS

The dynamic deflection experienced by the pipe and restraint is calculated using the model in Figure 3 and the PWRRA program (Reference 3). The pipe parameters used in the analysis are summarized in the figure. The effecitve pipe break force time history, F(t), is shown in Figure 4. PWRRA computes the nonlinear time history response of the pipe and the restraint system.

The model in Figure 3 considers the restraint SI3R-640A as a bilinear spring element with an initial gap. The load deflection characteristic of this bilinear spring was derived from an independent static finite element analysis, including geometric and material nonlinearities of the restraint SI3R-640A.

The ADINA program (Reference 4) was used to compute the bilinear spring characteristics. Figure 5 shows the ADINA model in the restraint plane. The main features of the finite element model are summarized below with reference to the node numbers shown on Figure 5. Further details of the model and computer output are contained in SAD Calculations 8.15.1-14.

A. Beam elements with elastic-plastic material behavior are used to represent the tension rod, the column under honeycomb, and gusset plates, which are not in the Y-Z plane. Table 1 summarizes the yield strength values used for these elements.

B. Elastic-plastic plane stress elements in the Y-Z plane are used to model the honeycomb (EAM) material and the gusset plate above the honeycomb. A yield strength equal to a crushing strength of 6 ksi was used for the honeycomb. Dynamic tests conducted on honeycomb material show that material crushing strength does not decrease significantly because of load angularity (Reference 2). The yield strength used for gusset plate elements is given in Table 1.

C. A series of radial gap elements with center at node number 17 (ring center) are connected to the ring perimeter nodal points where contact between pipe and ring will occur. The gap for radial element 17-16 located on the negative Y-axis is taken to be the effective gap of 1.754 inches. The gaps for other elements are taken as this gap plus the geometric gap dictated by the undeformed surface of pipe and ring. The spring constant for gap elements was selected from a consideration of local stiffness of the pipe.

To obtain the load-deflection diagram for this restraint, a displacement δ_p is applied incrementally at node point 17 of Figure 5, and the corresponding force in radial elements is computed. This incremental analysis is carried out for a sufficient number of steps using the large displacement option of the ADINA program to obtain the restraint load-deflection curve as shown in Figure 6.

IV. SUMMARY OF RESULTS

The restraint reaction is plotted against the pipe deflection in Figure 6. The calculated data points are idealized by the bilinear diagram shown in the figure. This is the required bilinear spring characteristic for use in the PWRRA model (Figure 3). Note that restraint reaction is zero prior to closing of the effective gap.

Also shown in Figure 6 are the pipe displacement values at which EAM begins to crush and the tension rods yield.

The displaced configuration of the restraint after 45 (δ_p = 2.525") and 75 (δ_p = 4.005") steps of static solution are shown in Figures 7 and 8 by dash lines. In these figures, solid lines show the undeformed configuration.

When the bilinear load deflection curve of Figure 6 is used in the dynamic model of Figure 3, the maximum pipe deflection needed to accommodate the pipe break time history of Figure 4 is calculated to be 3.15 inches. This maximum deflection is marked in Figure 6.

Figure 9 shows the deformation of the honeycomb needed to accommodate the pipe break. Figure 10 shows the tension leg force versus the pipe deflection. Note that the tension leg is in tension at all load levels and thus the question of buckling of tension rod does not arise. The strains in the honeycomb, tension rods and pipe at the maximum pipe deflection are shown in Figure 6. Since strain in the EAM, tension rods and pipe at the maximum deflection are within the acceptable limits, it is concluded that SI3R-640A can withstand the critical pipe break force which is postulated to occur.

V. REFERENCES

1. Letter from B. J. Youngblood of NRC to D. L. Farrar of CECo, dated July 21, 1983; Enclosure 1.

2. Commonwealth Edison Co, "Evaluation of Energy-Absorbing Material for Pipe Whip Restraints," Report No. SAD-431, Revision 1, April 1984.

3. Sargent & Lundy, "Pipe Whip Restraint Reaction Analysis Program-PWRRA, Program No. 09.5.125-2.1Ø.

4. ADINA Engineering, "Automatic Dynamic Incremental Nonlinear Analysis - ADINA," S&L Program No. 09.7.199-2.0Ø.

TABLE 1 VALUES OF YIELD STRENGTH
FOR VARIOUS STEEL ELEMENTS
(Section III, Items A and B)

Component	Yield Strength (ksi)
Tension Rod	112.0
Gusset Plates	56.2
W 8 x 35	56.2

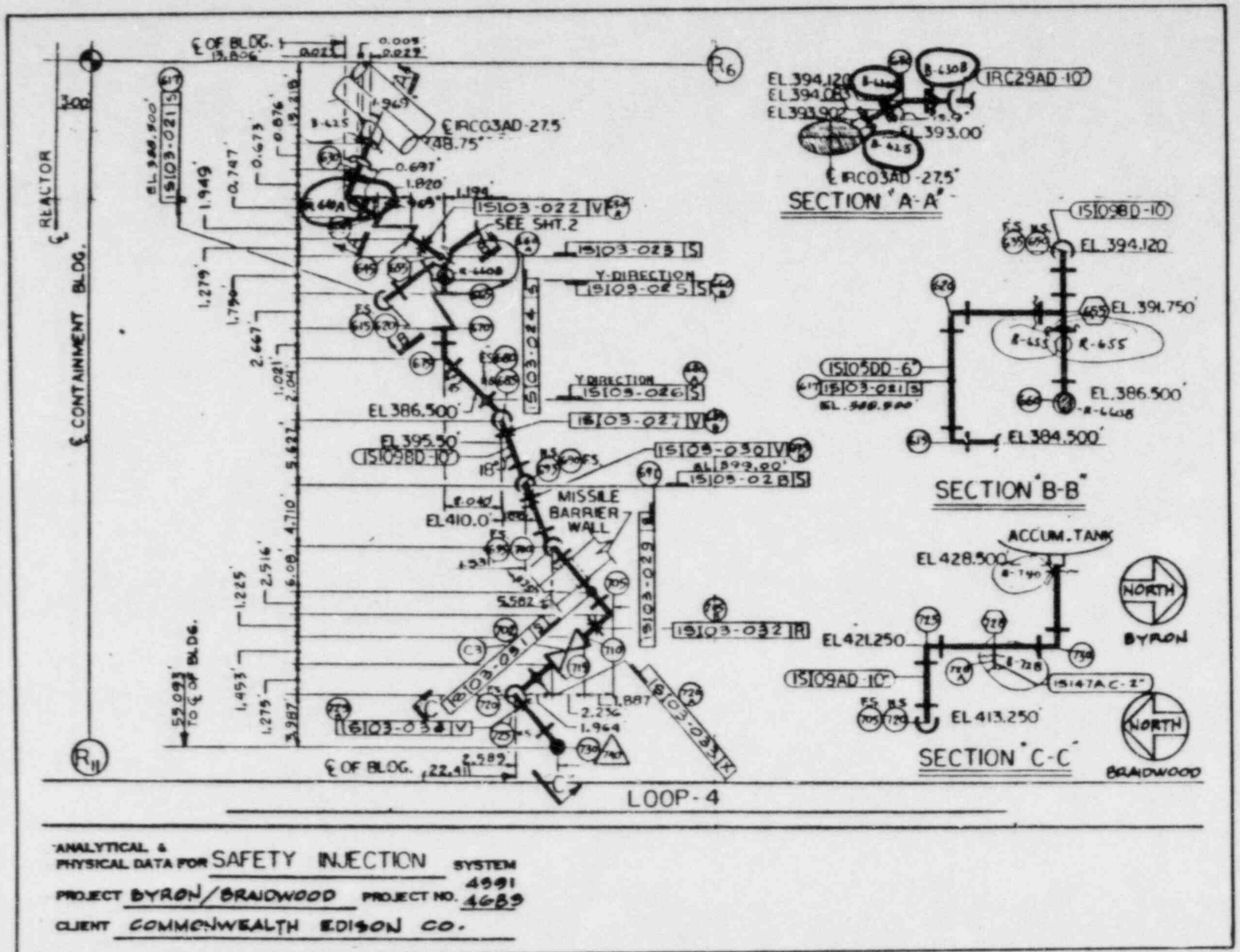

LOCATIONS OF RESTRAINT S13R-640A AND BREAKS B-625, B-630A AND B-630B

FIGURE 1

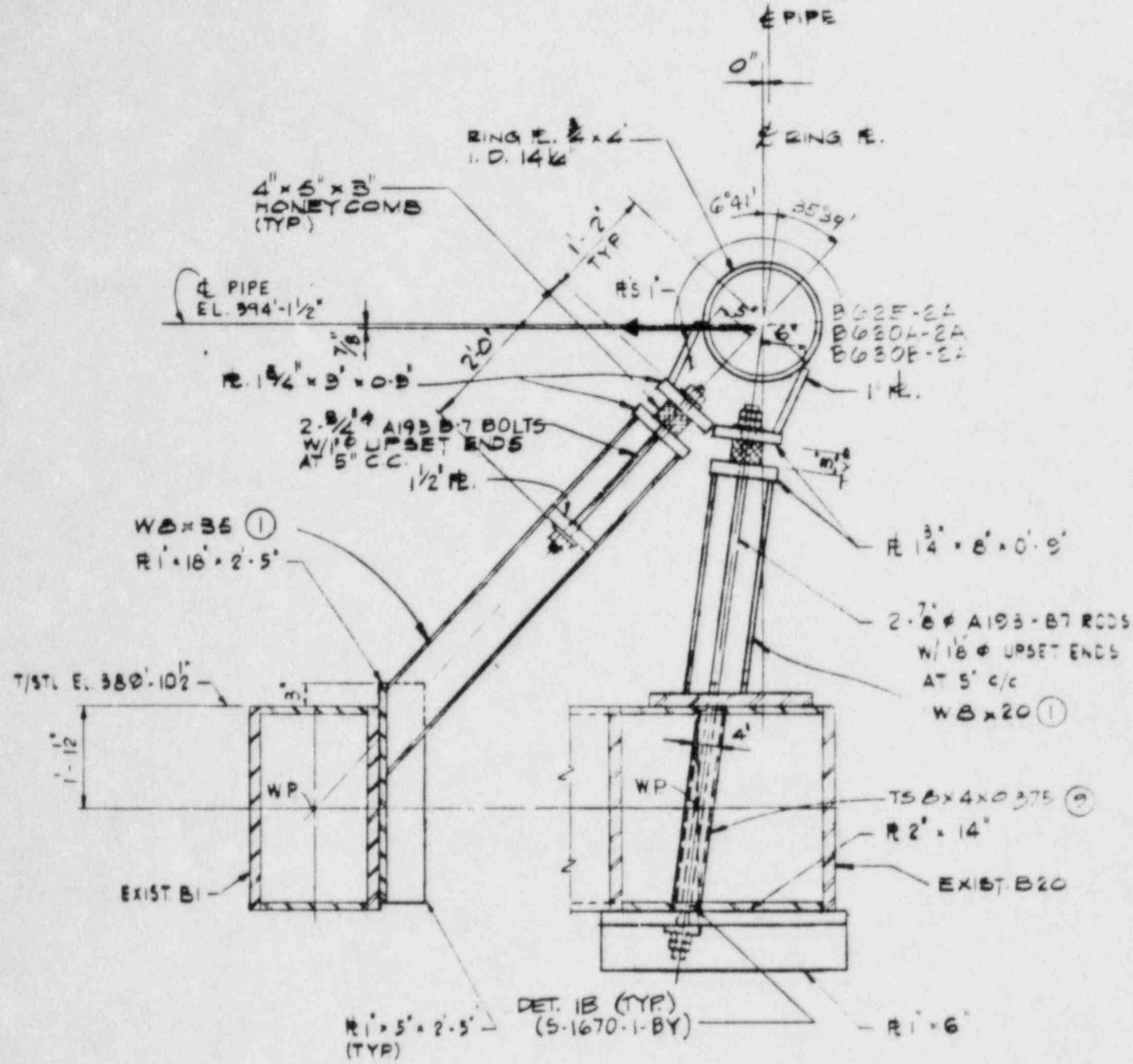

RESTRAINT SI3R-640A

FIGURE 2

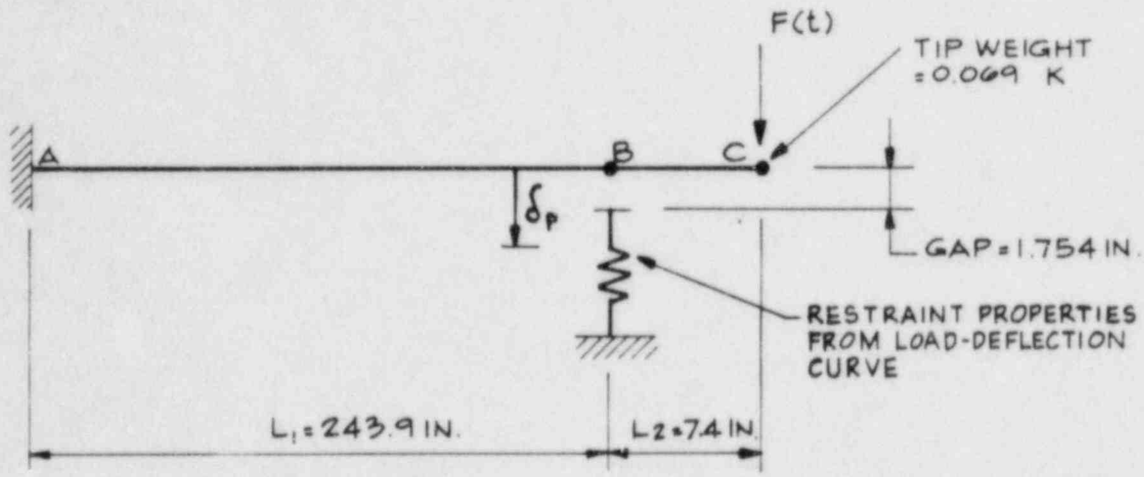

PIPE PROPERTIES:

WEIGHT	= 0.01171 K/IN.
O.D.	= 10.75 IN.
THICKNESS	= 1.0 IN.
YIELD STRESS	= 28.7 KSI
ULTIMATE STRESS	= 62.0 KSI
ELASTICITY MODULUS	= 27,500 KSI

PIPE WHIP RESTRAINT MODEL USED FOR DYNAMIC ANALYSIS OF S13R-640A

FIGURE 3

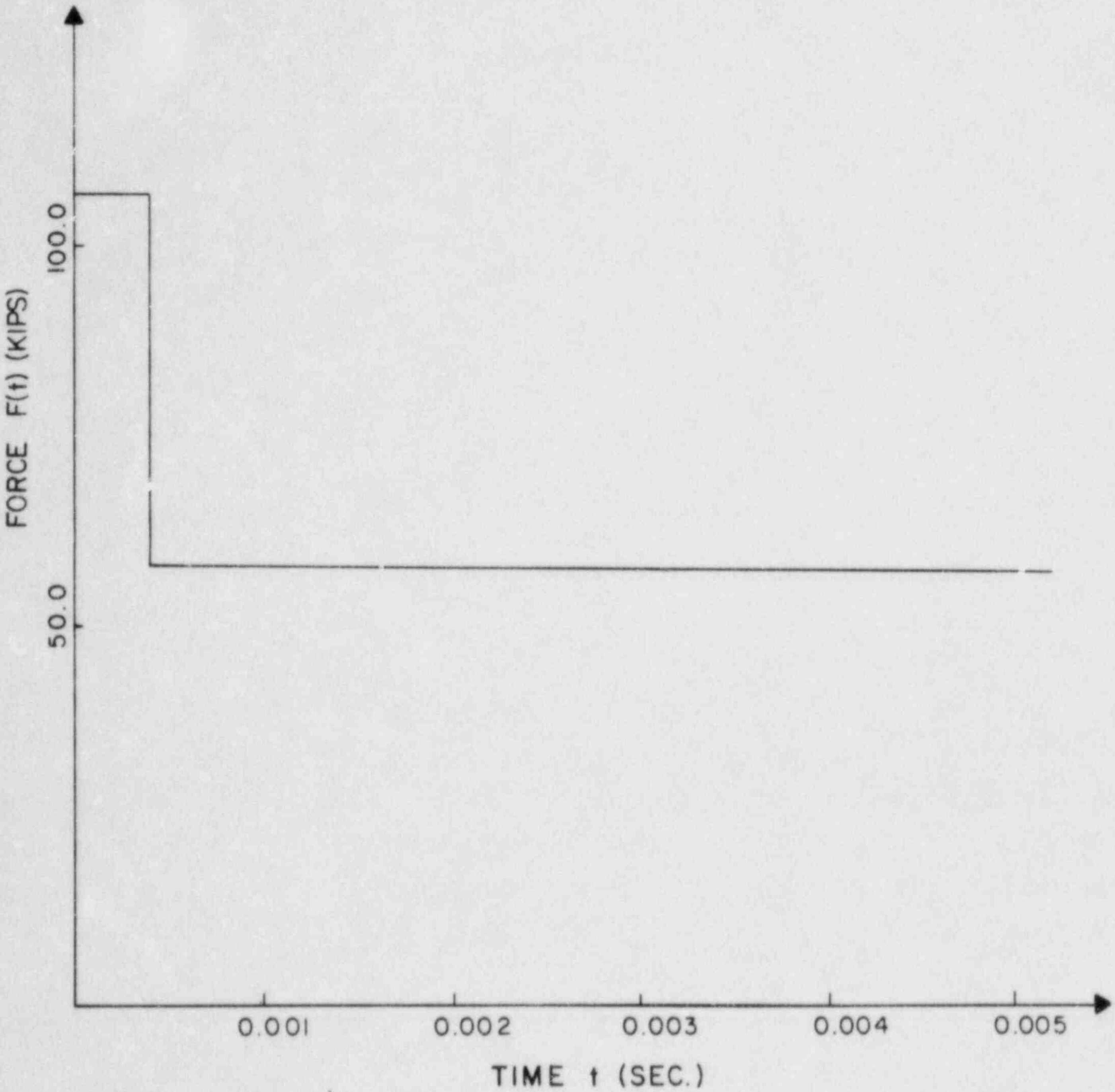

FORCE TIME HISTORY OF PIPE BREAKS B-625-2A, B-630A-2A & B-630B-2A

FIGURE 4

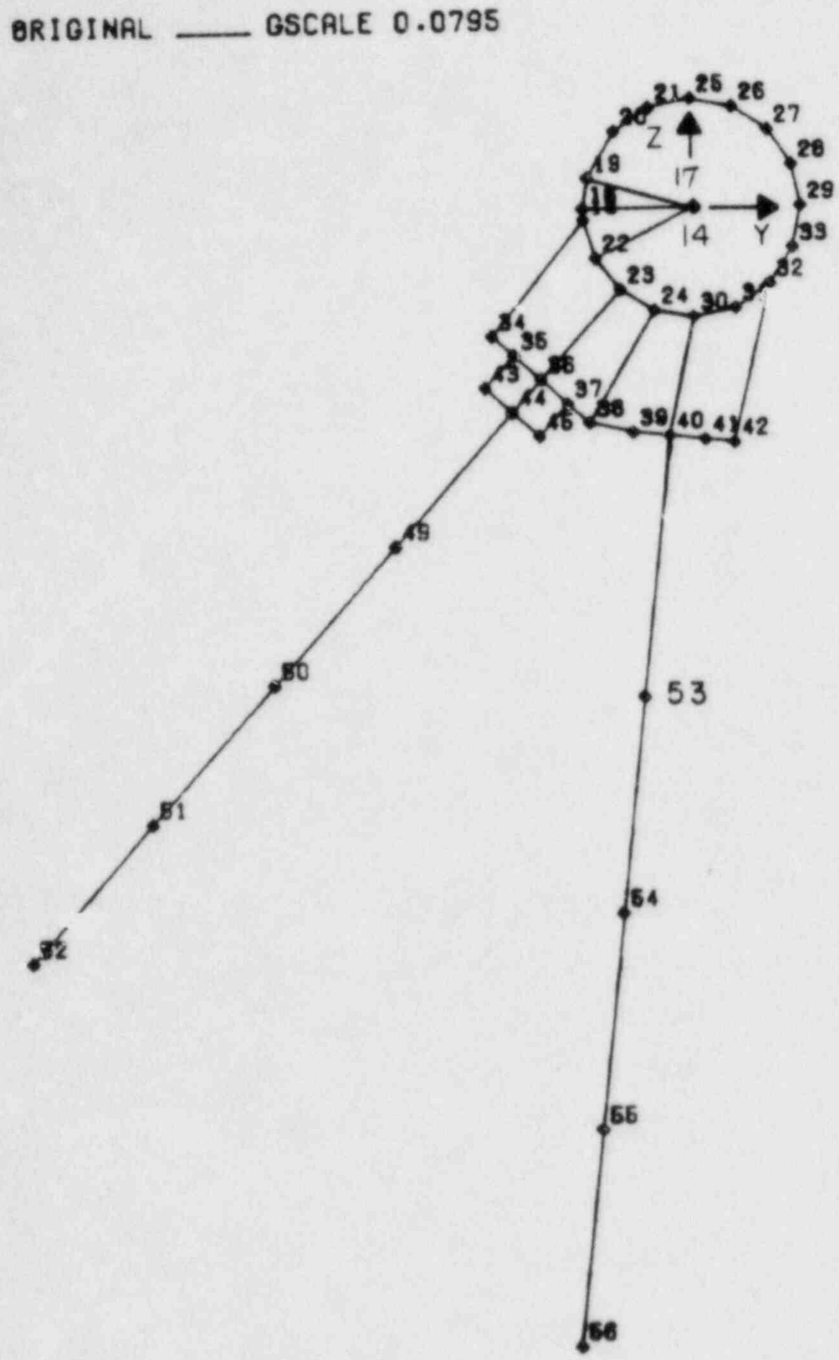

VIEW OF FINITE ELEMENT MODEL IN PLANE OF RESTRAINT SI3R-640A

FIGURE 5

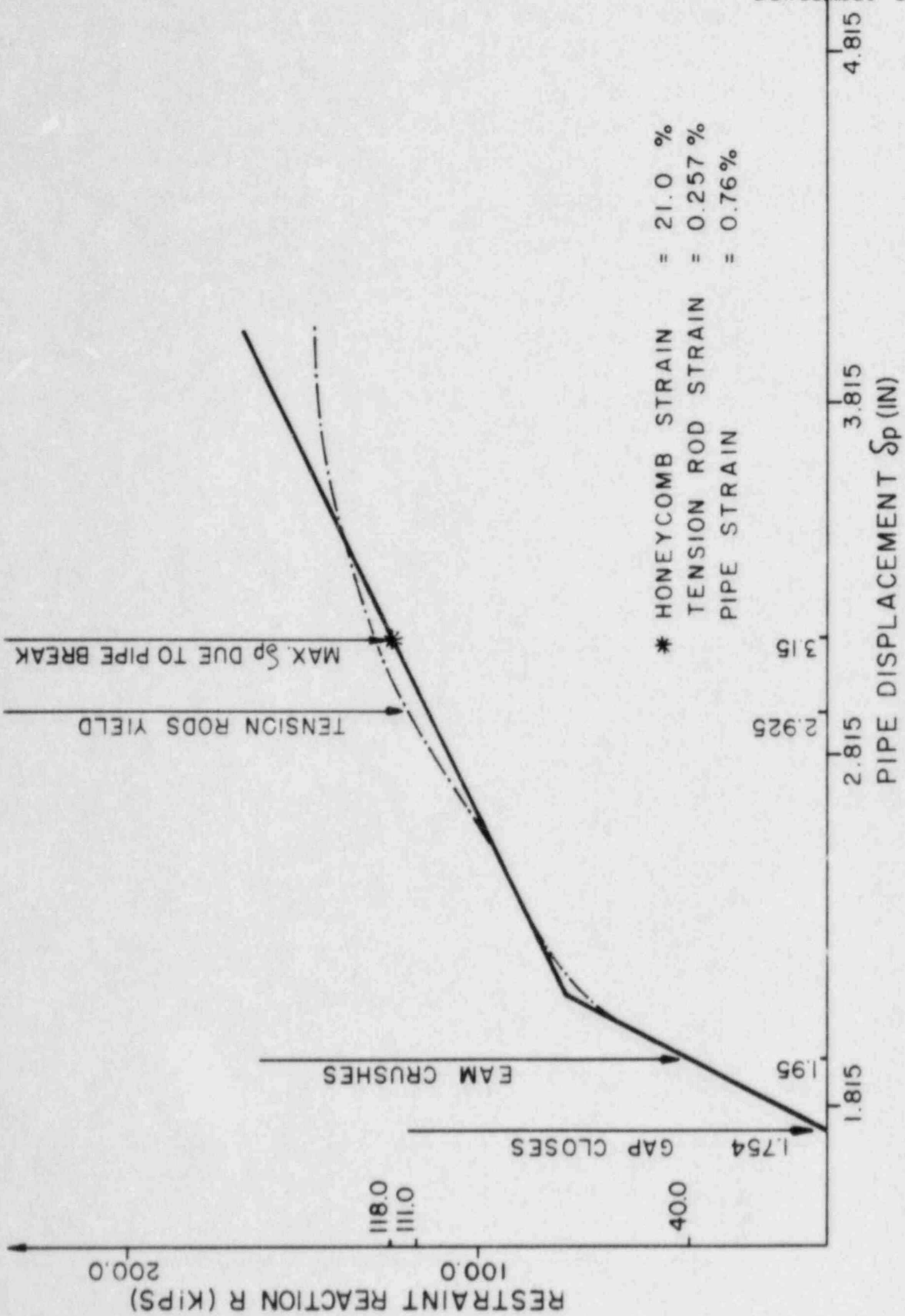

LOAD-DEFLECTION CURVE FOR SI3R-640A

FIGURE 6

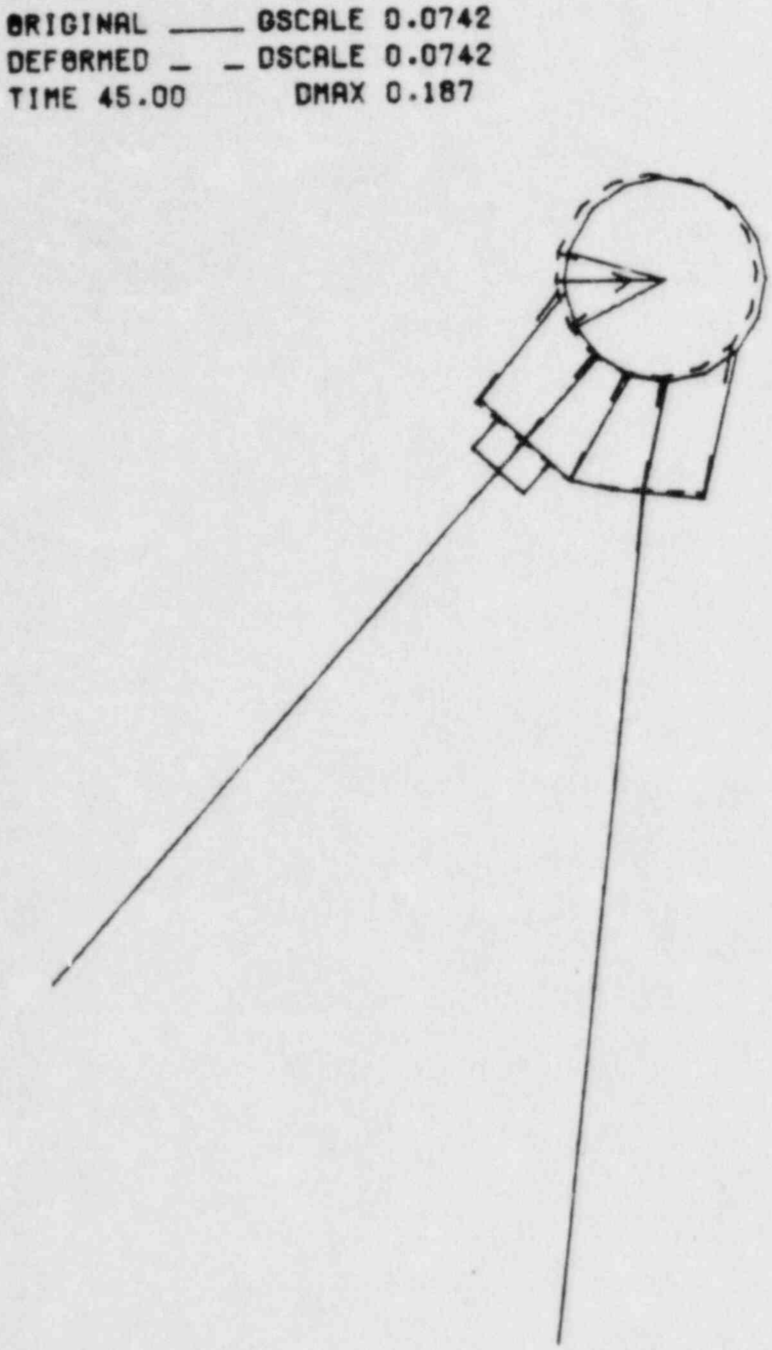

DISPLACED CONFIGURATION OF
RESTRAINT S13R-640A AT δ_p = 2.525 IN.

FIGURE 7

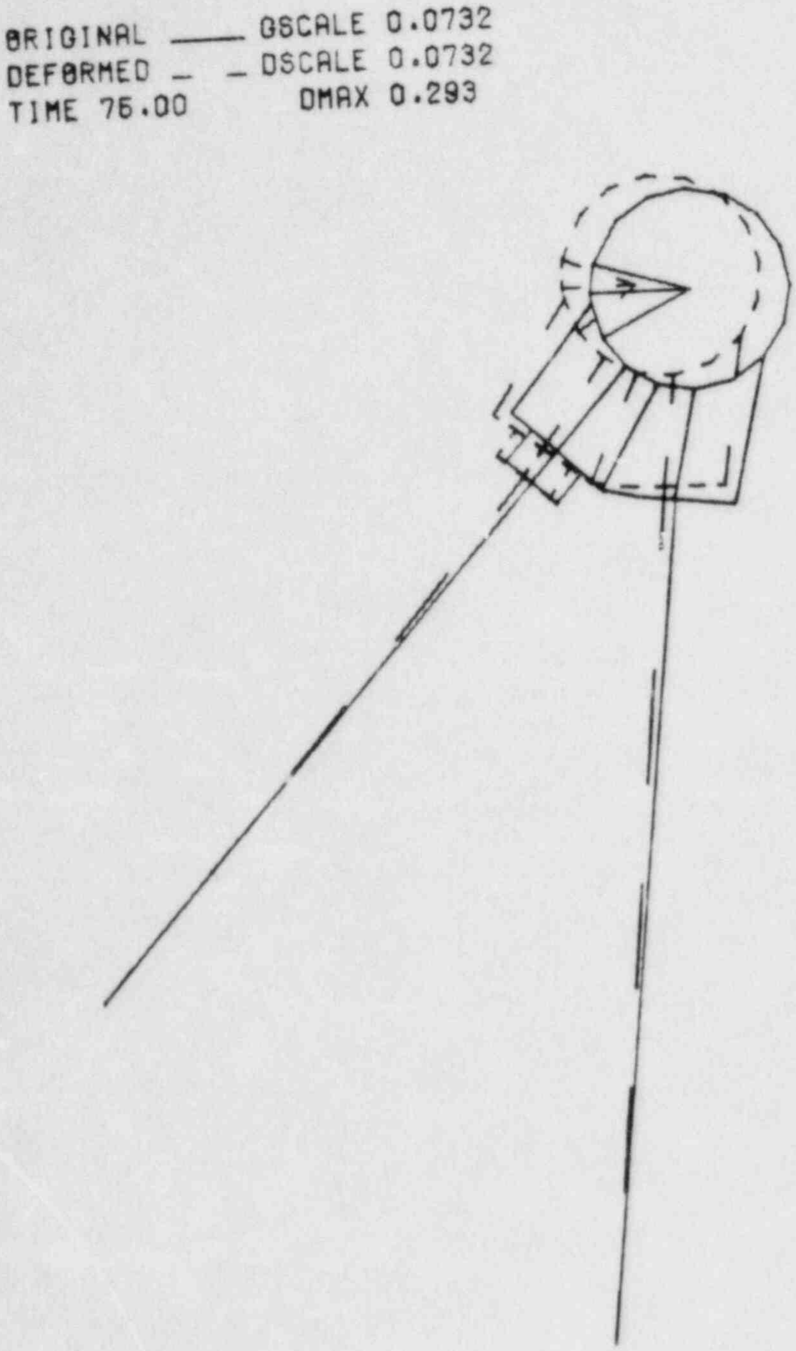

DISPLACED CONFIGURATION OF
RESTRAINT SI3R-640A AT δ_p = 4.0 IN.

FIGURE 8

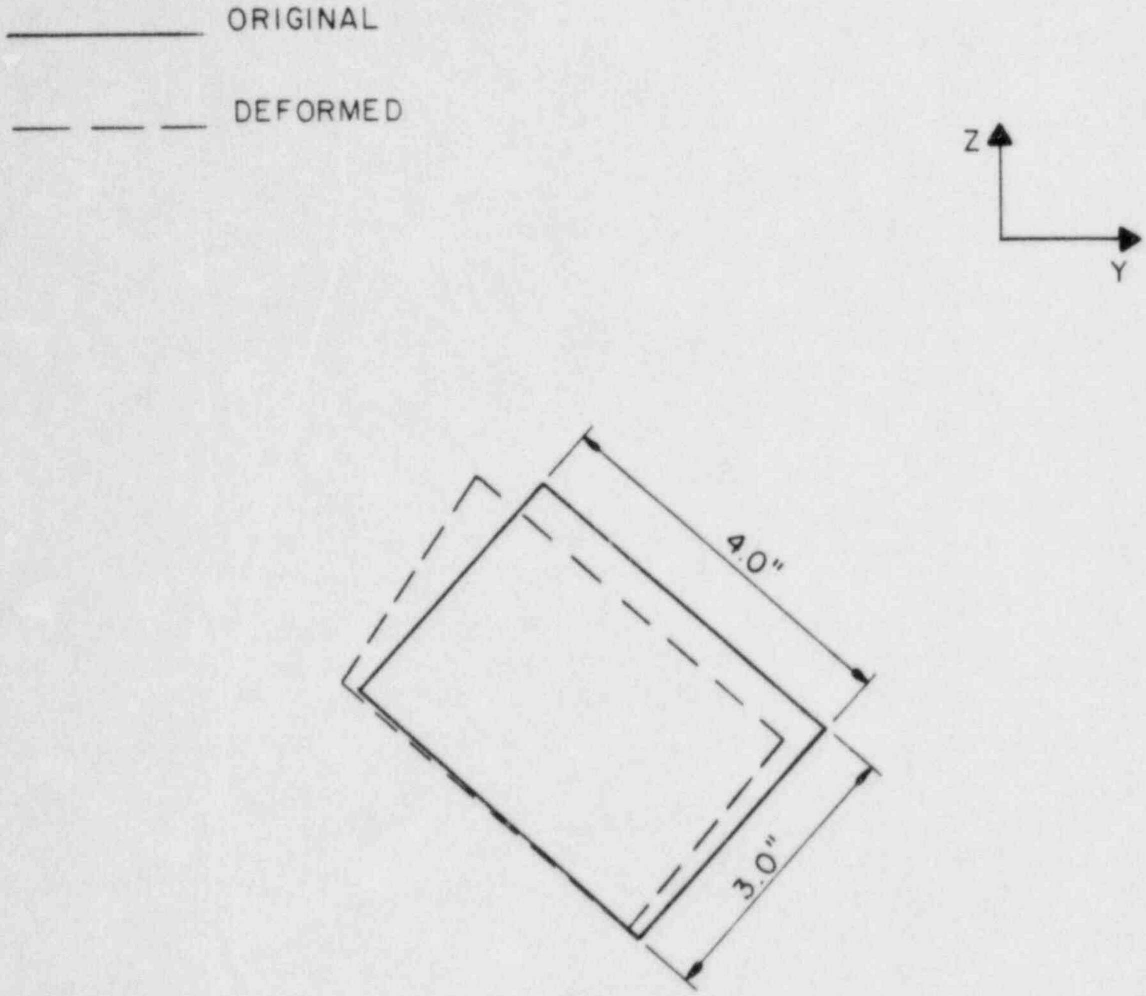

DISPLACED CONFIGURATION OF EAM AT MAX δ_p DUE TO PIPE BREAK

FIGURE 9

15

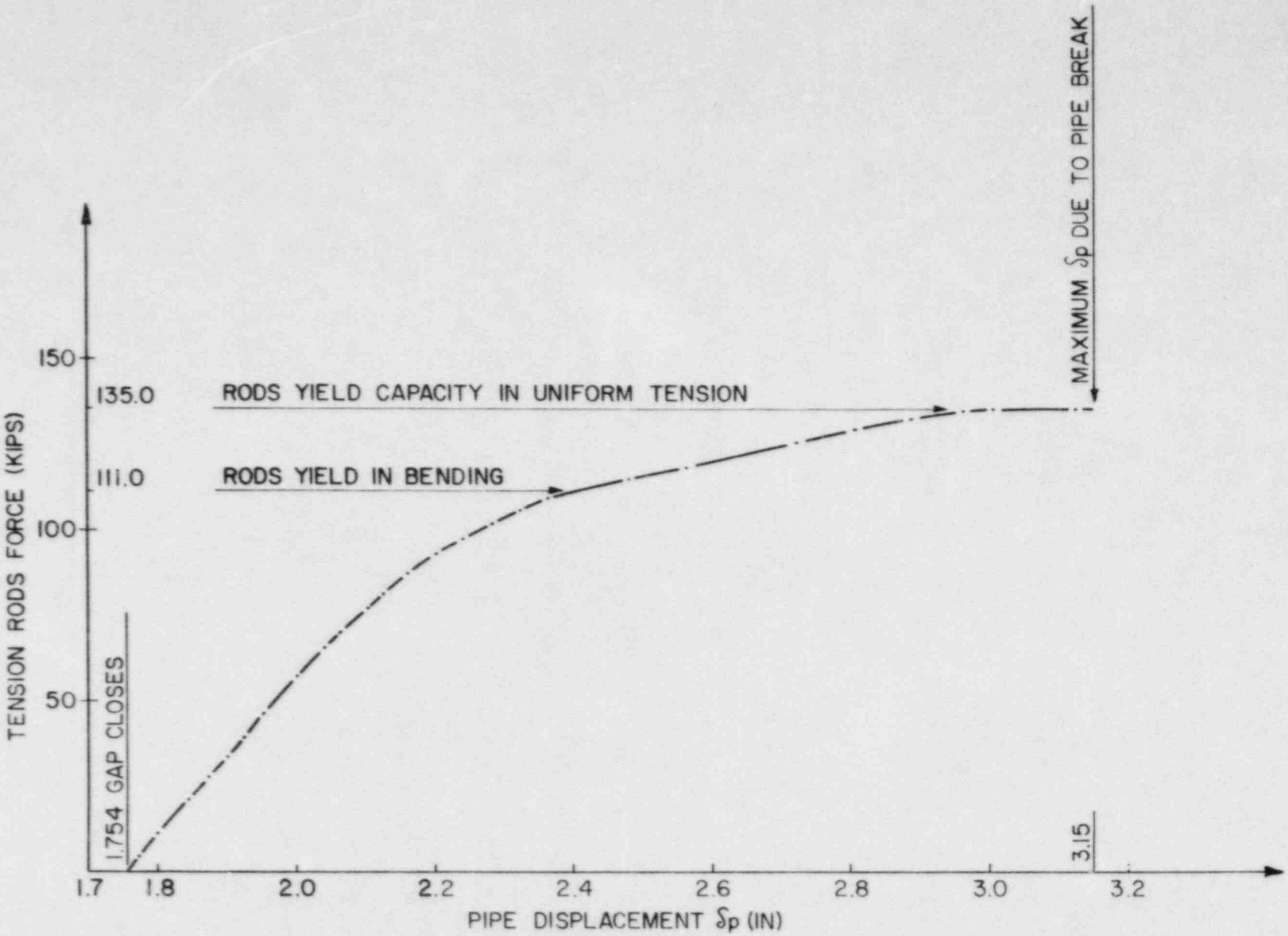

TENSION RODS FORCE VS. PIPE DISPLACEMENT FOR SI3R-640A

FIGURE 10

APPENDIX A

Summary of Results for Deleted Restraint FWR-35

Figure A1 and A2 show the location and construction of pipe whip restraint FWR-35. As discussed in Section I this restraint is no longer needed because of changes in break locations. The discussion below assumes break locations which would have required the restraint. This restraint was designed to resist break force B-80A. The location of the break is marked in Figure A1 and the direction of the force on the restraint is shown in Figure A2.

Figures A3 and A4 show the dynamic analysis model and forcing function. The finite element model for static load deflection is shown in Figure A5.

The restraint reaction is plotted against the pipe deflection in Figure A6. The calculated data points are idealized by the bilinear diagram shown in the figure. This is the required load-deflection diagram for use in the PWRRA model in Figure A3. Note that restraint reaction is zero prior to closing of the effective gap. Also shown in Figure A6 are the pipe displacement values at which the tension rod yields and EAM begins to crush.

The displaced configuration of the restraint after 70 (δ_p = 3.25") steps of static solution is shown in Figure A7 by dashed lines. In this figure, solid lines show the undeformed configuration.

When the bilinear load deflection diagram of Figure A6 is used in the dynamic model of Figure A3, the maximum pipe deflection needed to accommodate the pipe break time history of Figure A4 is calculated to be 2.87 inches. This maximum deflection is marked in Figure A6. Figure A8 shows the deformation of the EAM needed to accommodate the pipe break force. Figure A9 shows the tension rod force versus the pipe deflection. Note that the tension rod is in tension at all load levels and thus the question of buckling of tension rod does not arise. The strains in the honeycomb, tension rod and pipe at the maximum pipe deflection are shown in Figure A6. Since the calculated strains in the EAM, tension rod and pipe at the maximum pipe deflection are within acceptable limits, it is concluded that FWR-35 can withstand the pipe break force which was postulated to occur.

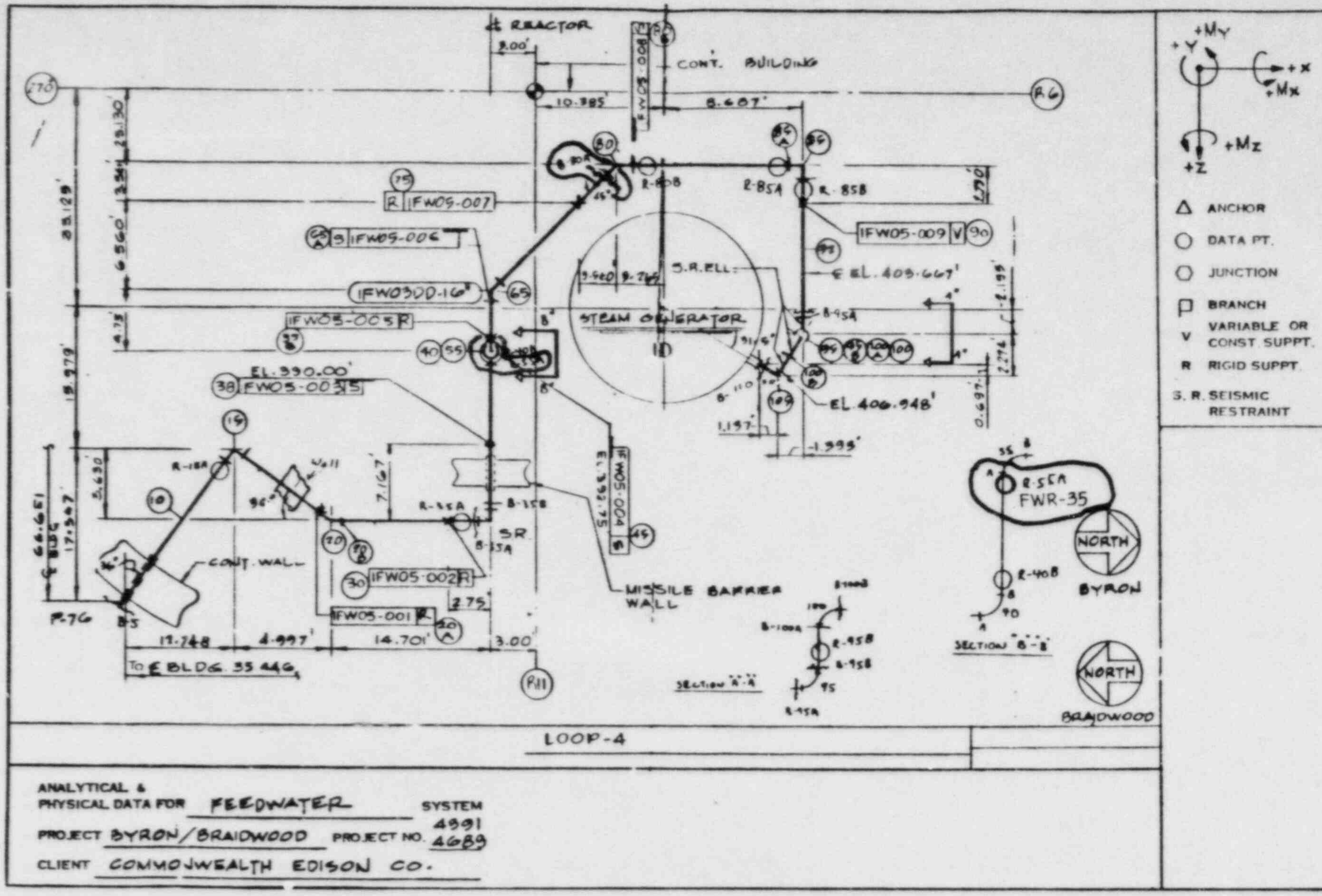

LOCATIONS OF RESTRAINT FWR-35 AND BREAK B-80A

FIGURE A1

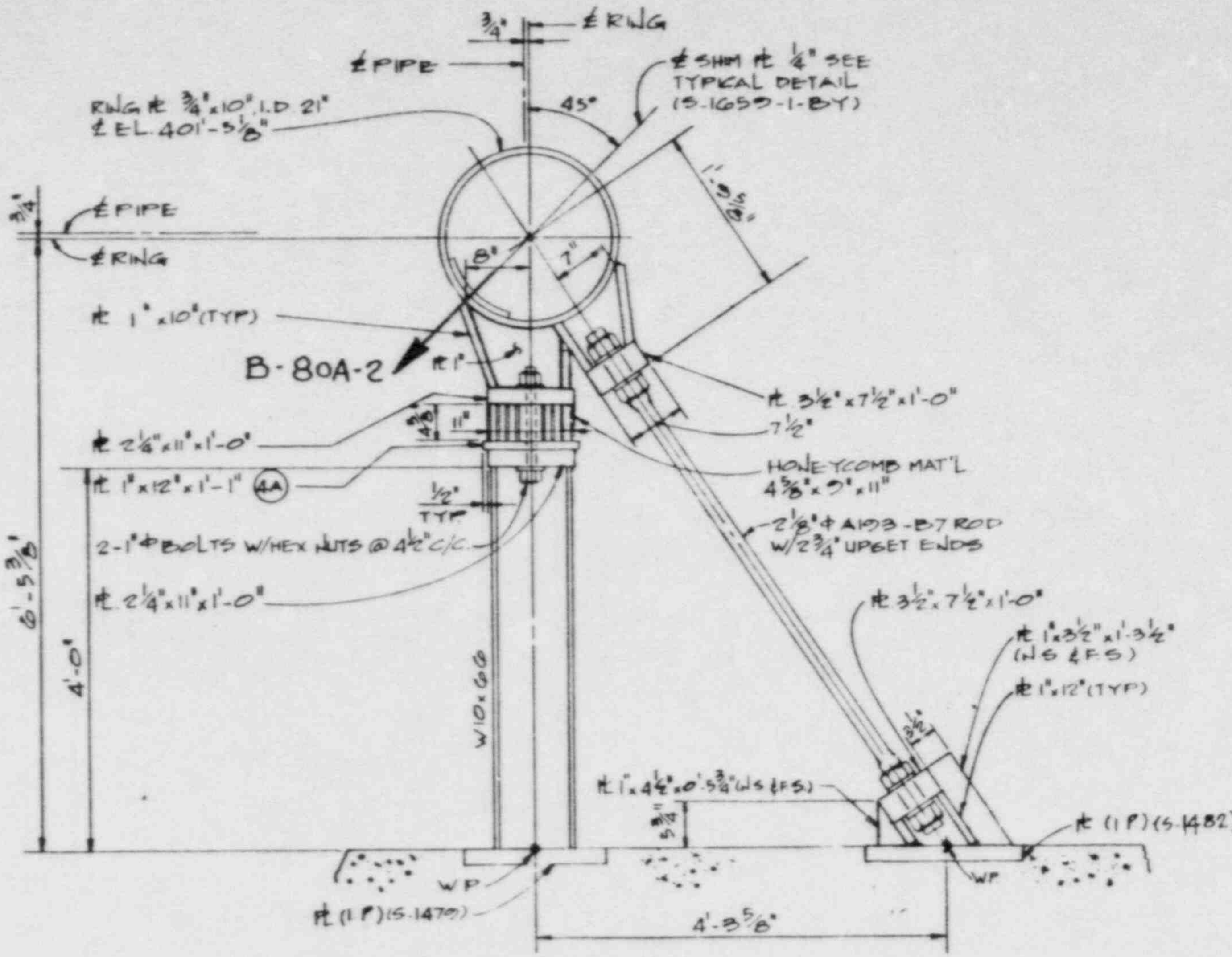

RESTRAINT FWR-35

FIGURE A2

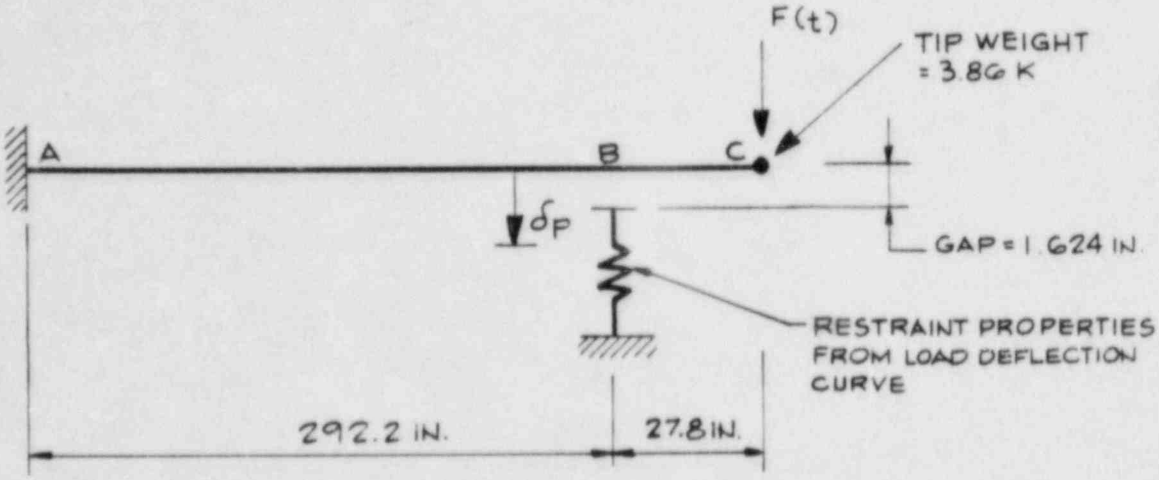

PIPE WEIGHT = 0.0182 K/IN.
O.D. = 16 IN.
THICKNESS = 0.843 IN.
YIELD STRESS = 28.9 KSI
ULTIMATE STRESS = 61.8 KSI
ELASTICITY MODULUS = 29000 KSI

PIPE WHIP RESTRAINT MODEL
USED FOR DYNAMIC ANALYSIS OF FWR-35

FIGURE A3

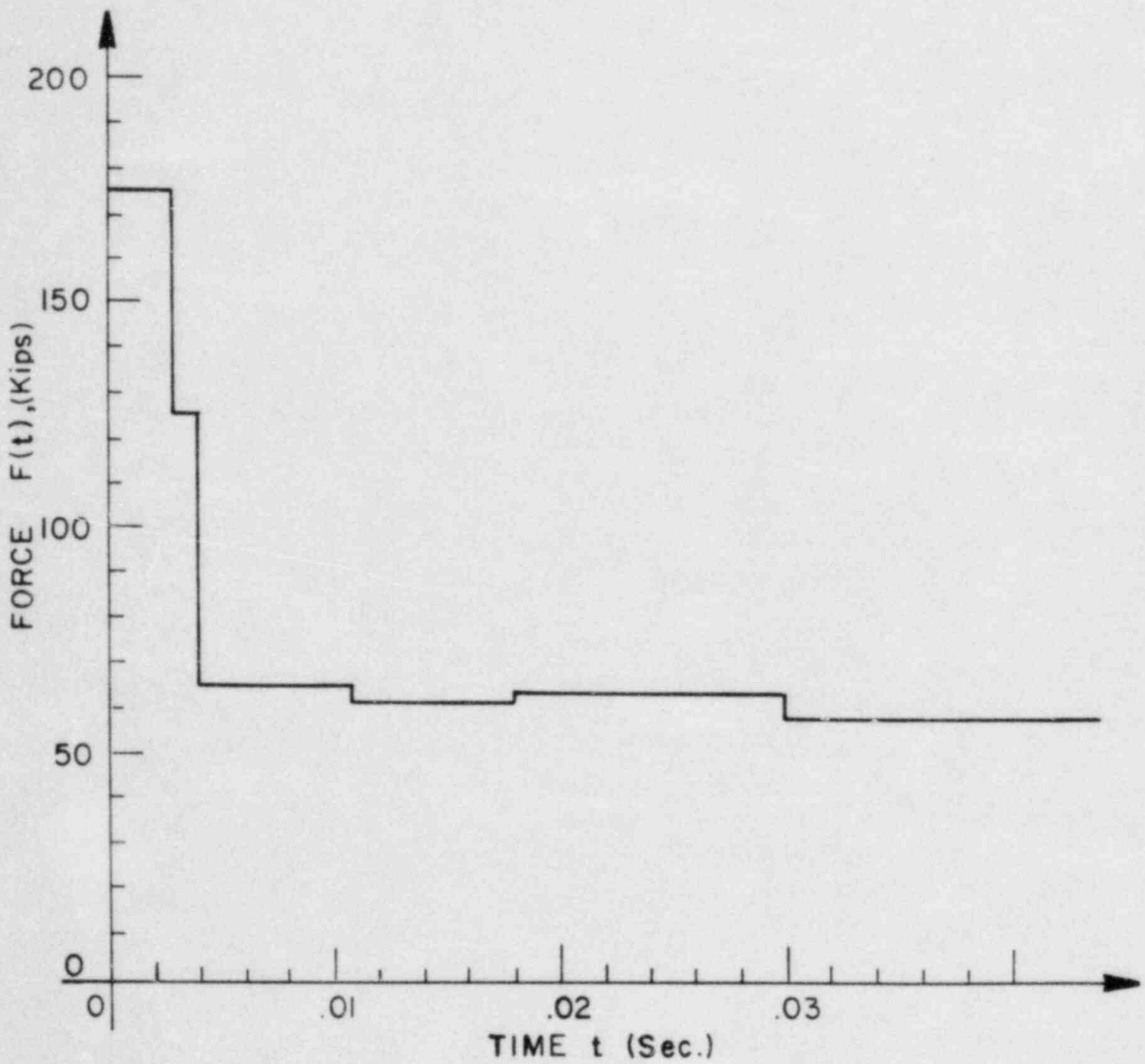

A-6

FORCE TIME HISTORY OF PIPE BREAK B-80A-2

FIGURE A4

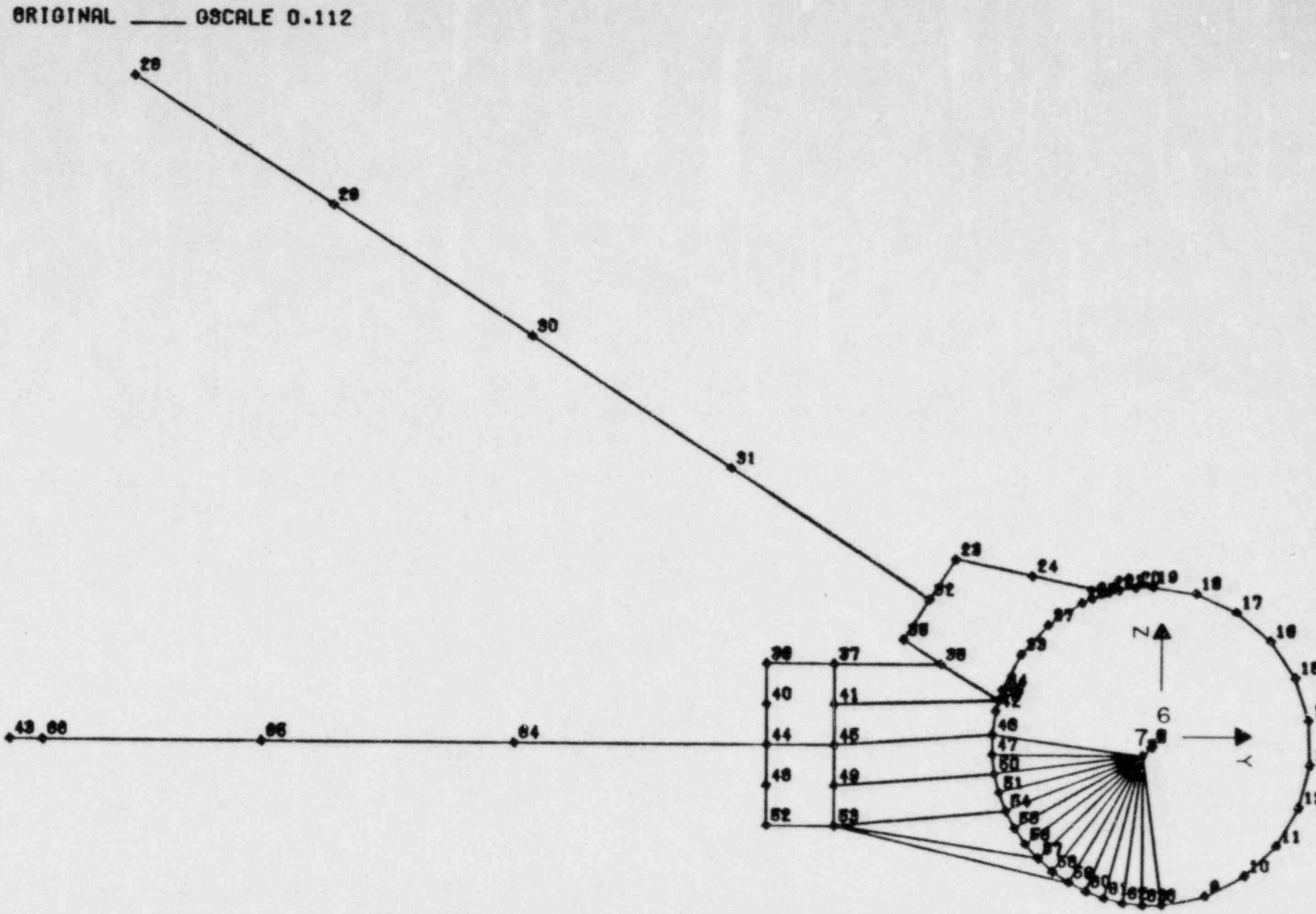

VIEW OF FINITE ELEMENT MODEL IN

PLANE OF RESTRAINT FWR-35

FIGURE A5

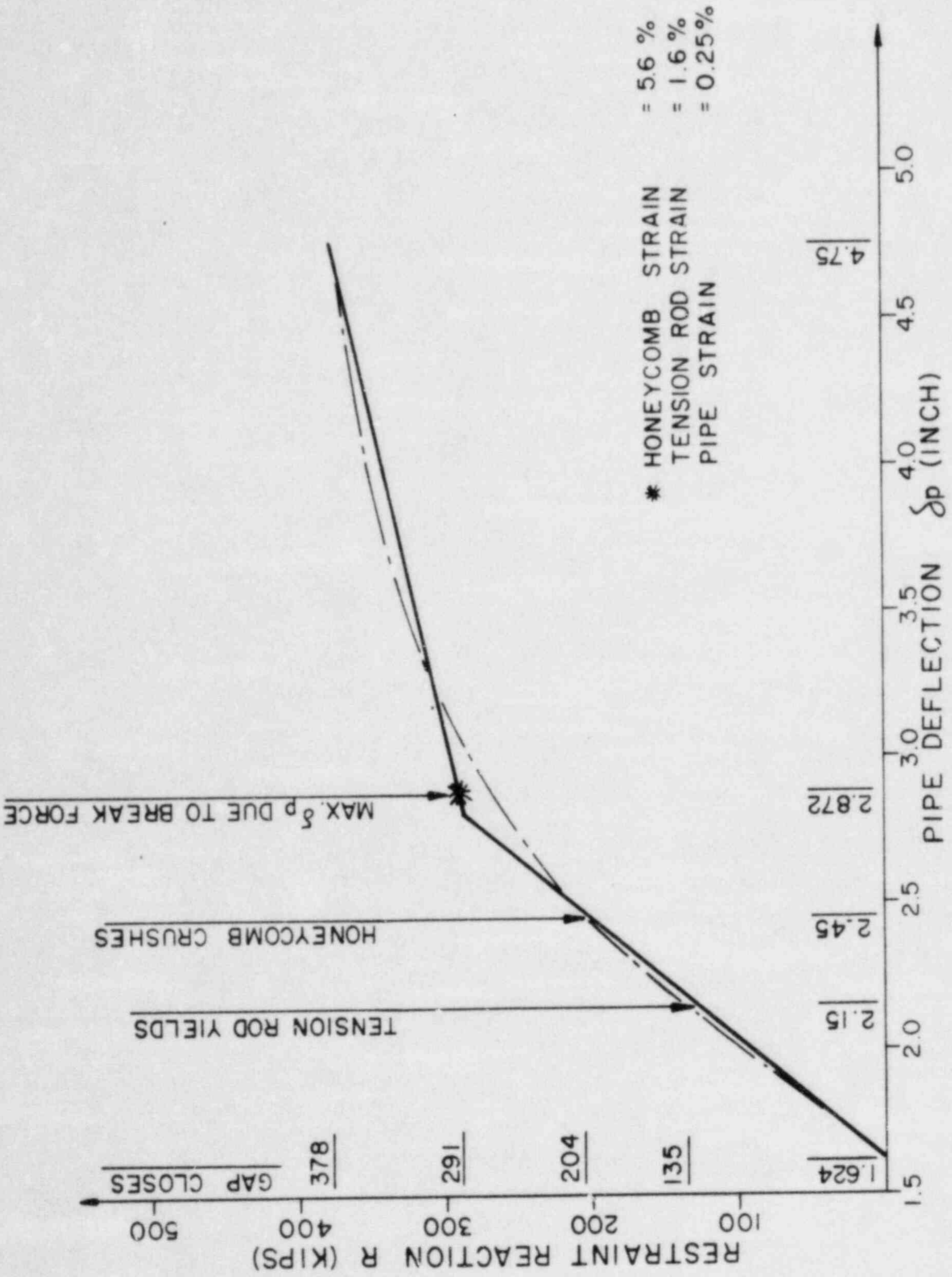

LOAD-DEFLECTION CURVE FOR FWR-35

FIGURE A6

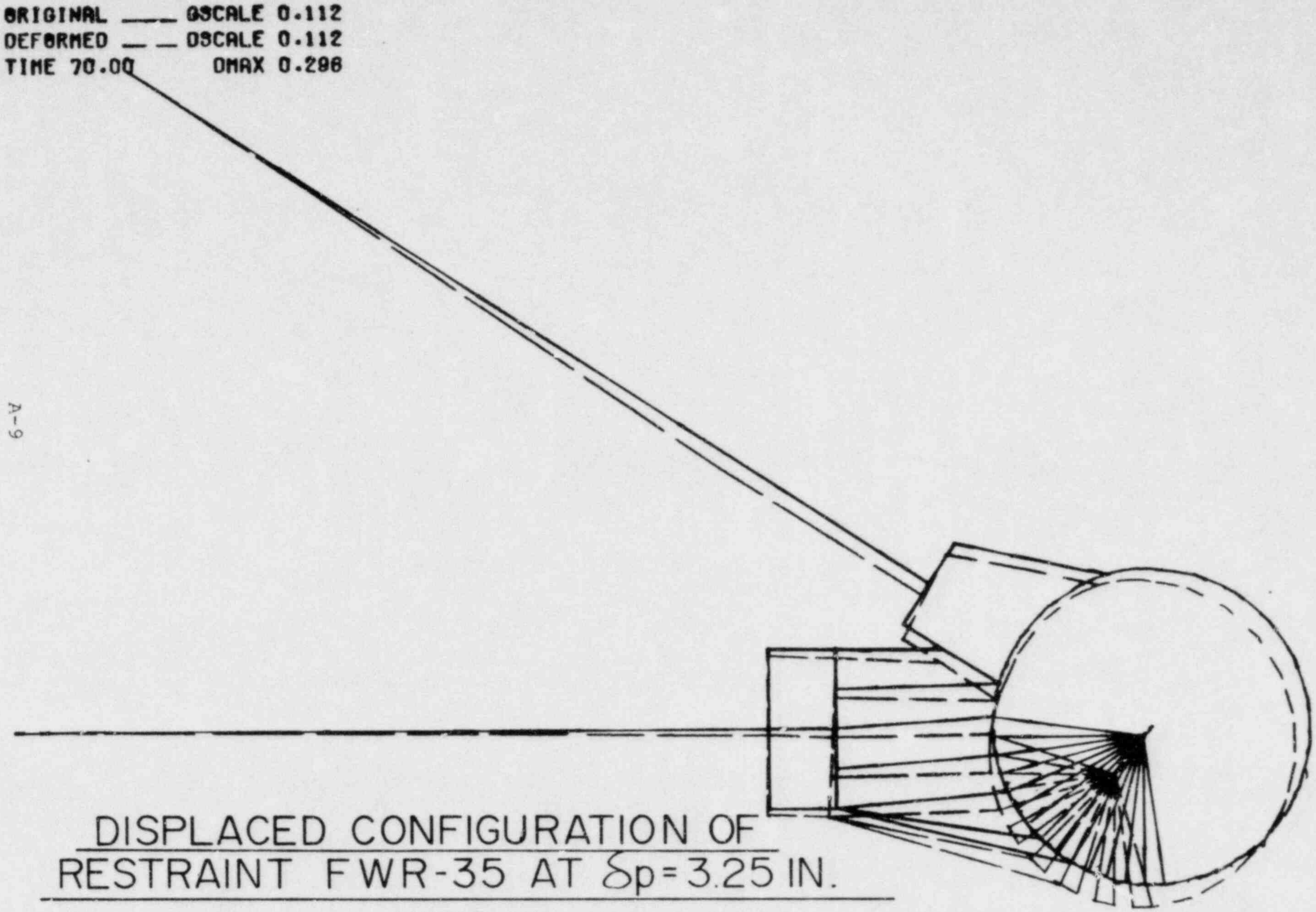

DISPLACED CONFIGURATION OF
RESTRAINT FWR-35 AT $\delta p = 3.25$ IN.

FIGURE A7

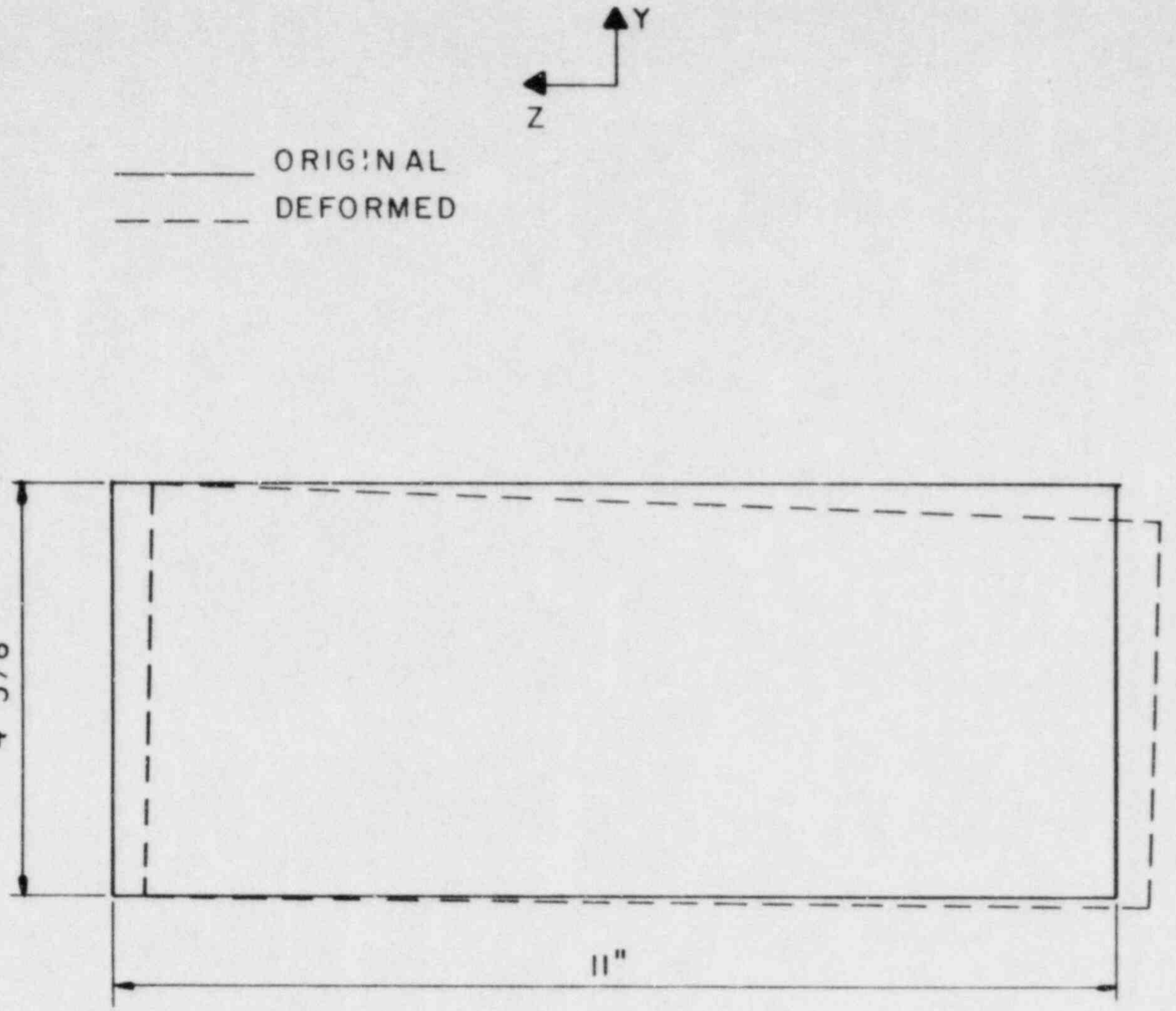

DISPLACED CONFIGURATION OF EAM FOR FWR-35 AT MAXIMUM δ_p DUE TO PIPE BREAK

FIGURE A8

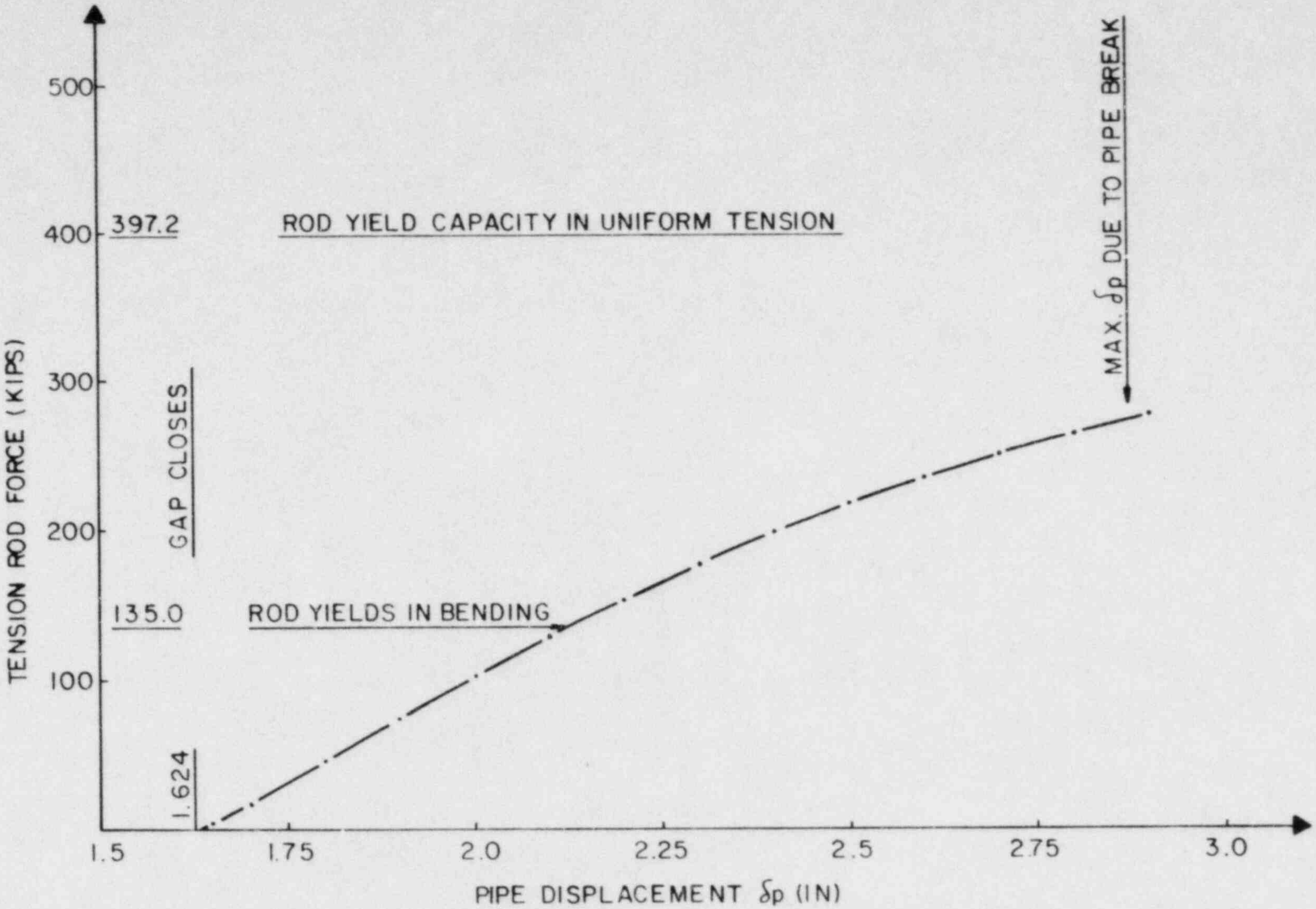

TENSION ROD FORCE VS. PIPE DISPLACEMENT

FIGURE A9

APPENDIX B

Summary of Results for Deleted Restraint FWR-16

Figures B1 and B2 show the location and construction of pipe whip restraint FWR-16. As discussed in Section I, this restraint is no longer needed because of changes in break locations. The discussion below assumes break locations which would have required the restraint. This restraint was designed to resist break force B-55A. The location of the break is marked in Figure B1 and the direction of the force on restraint is shown in Figure B2.

Figures B3 and B4 show the dynamic analysis model and forcing function. The finite element model for static load deflection is shown in Figure B5.

The restraint reaction is plotted against the pipe deflection in Figure B6. The calculated data points are idealized by the solid line shown in the figure. This is the required load-deflection diagram for use in the PWRRA (Figure B3). Also shown on Figure B6 are the pipe displacement values at which the tension rod yields and EAM begins to crush.

The displaced configuration of the restraint after 70 (δ_p = 3.12") steps of static solution is shown in Figure B7 by dashed lines. In this figure solid lines show the undeformed configuration.

When the linear load deflection diagram of Figure B6 is used in the dynamic model of Figure B3, the maximum pipe deflection needed to accommodate the pipe break time history of Figure B4 is calculated to be 2.544 inches. This maximum deflection is marked in Figure B6. Figure B8 shows the deformation of the EAM needed to accommodate the pipe break force. The strains in the honeycomb, tension rod and pipe at the maximum pipe deflection are shown in Figure B6. Since the calculated strains of the EAM, tension rod and pipe at the maximum pipe deflection are within acceptable limits, it is concluded that FWR-16 can withstand the critical pipe break force which was postulated to occur.

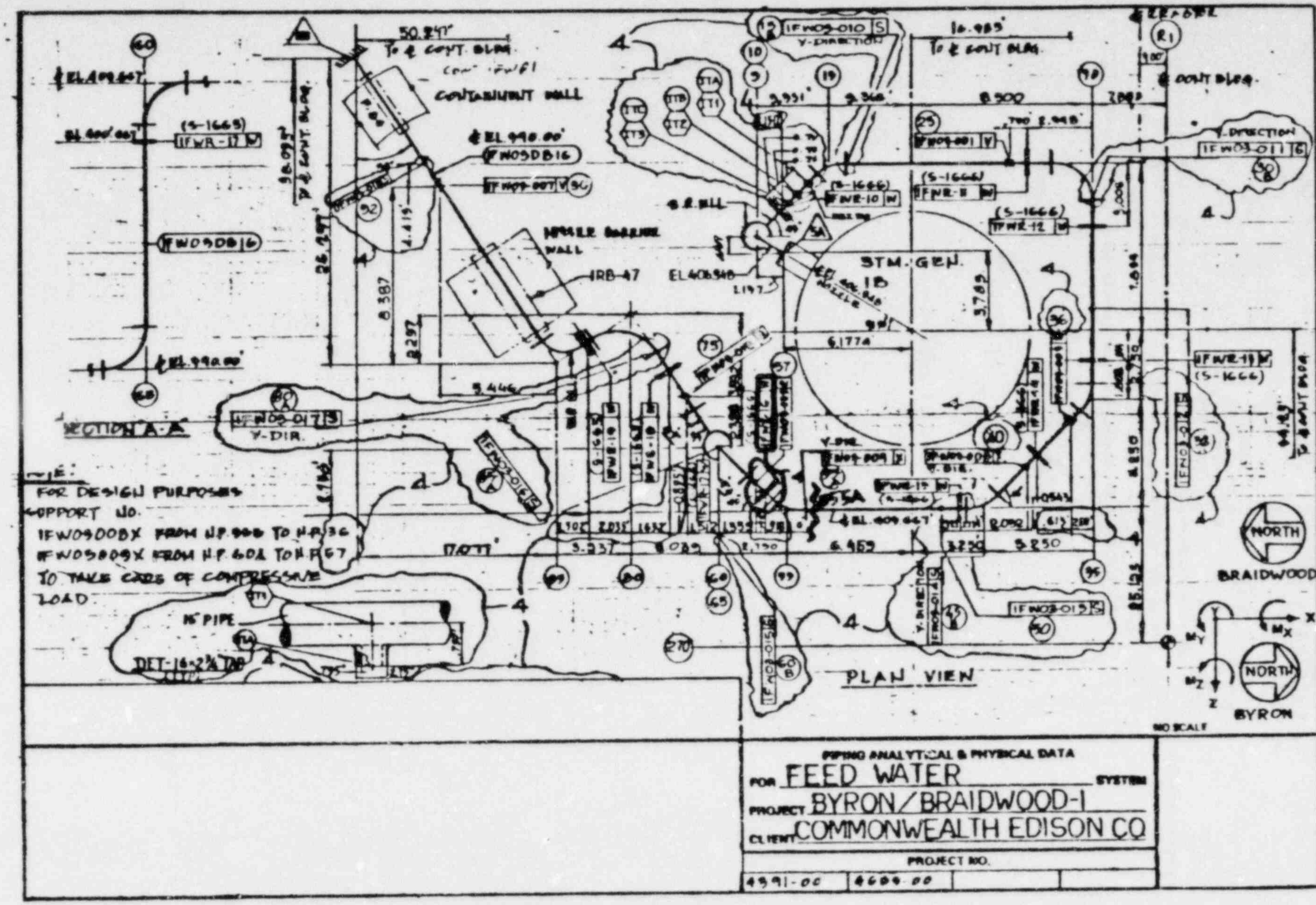

LOCATIONS OF RESTRAINT FWR-16 AND BREAK B-55A

FIGURE B1

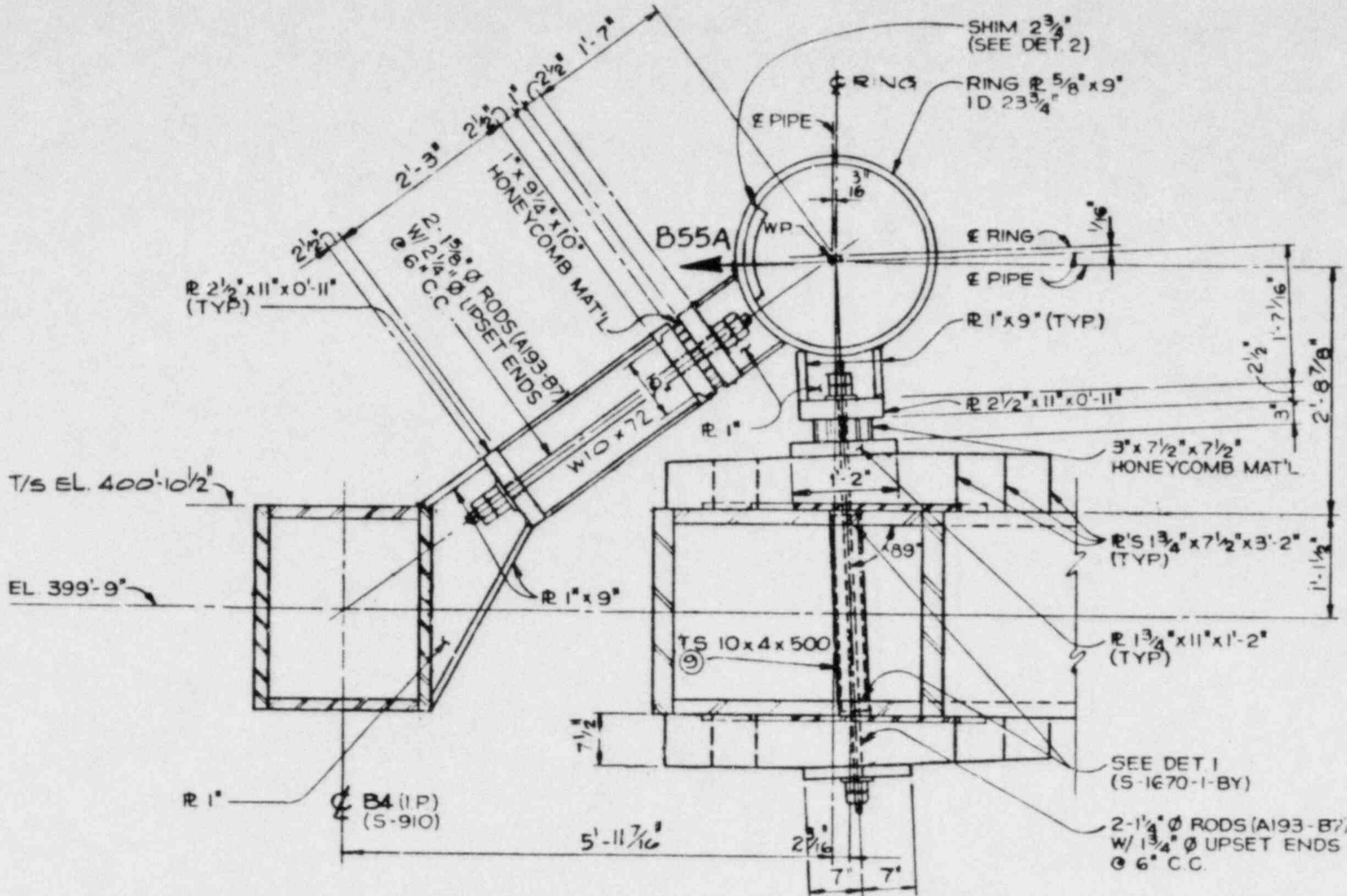

RESTRAINT FWR-16

FIGURE B2

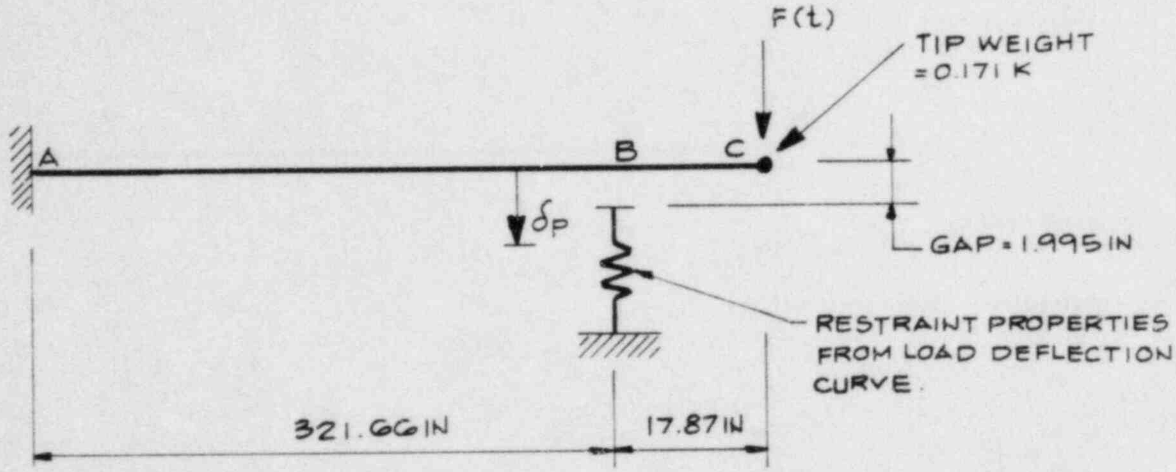

PIPE WEIGHT = 0.0182 K/IN
O.D. = 16 IN
THICKNESS = 0.843 IN
YIELD STRESS = 28.9 KSI
ULTIMATE STRESS = 61.8 KSI
ELASTICITY MODULUS = 29000.0 KSI.

PIPE WHIP RESTRAINT MODEL USED FOR DYNAMIC ANALYSIS OF FWR-16

FIGURE B3

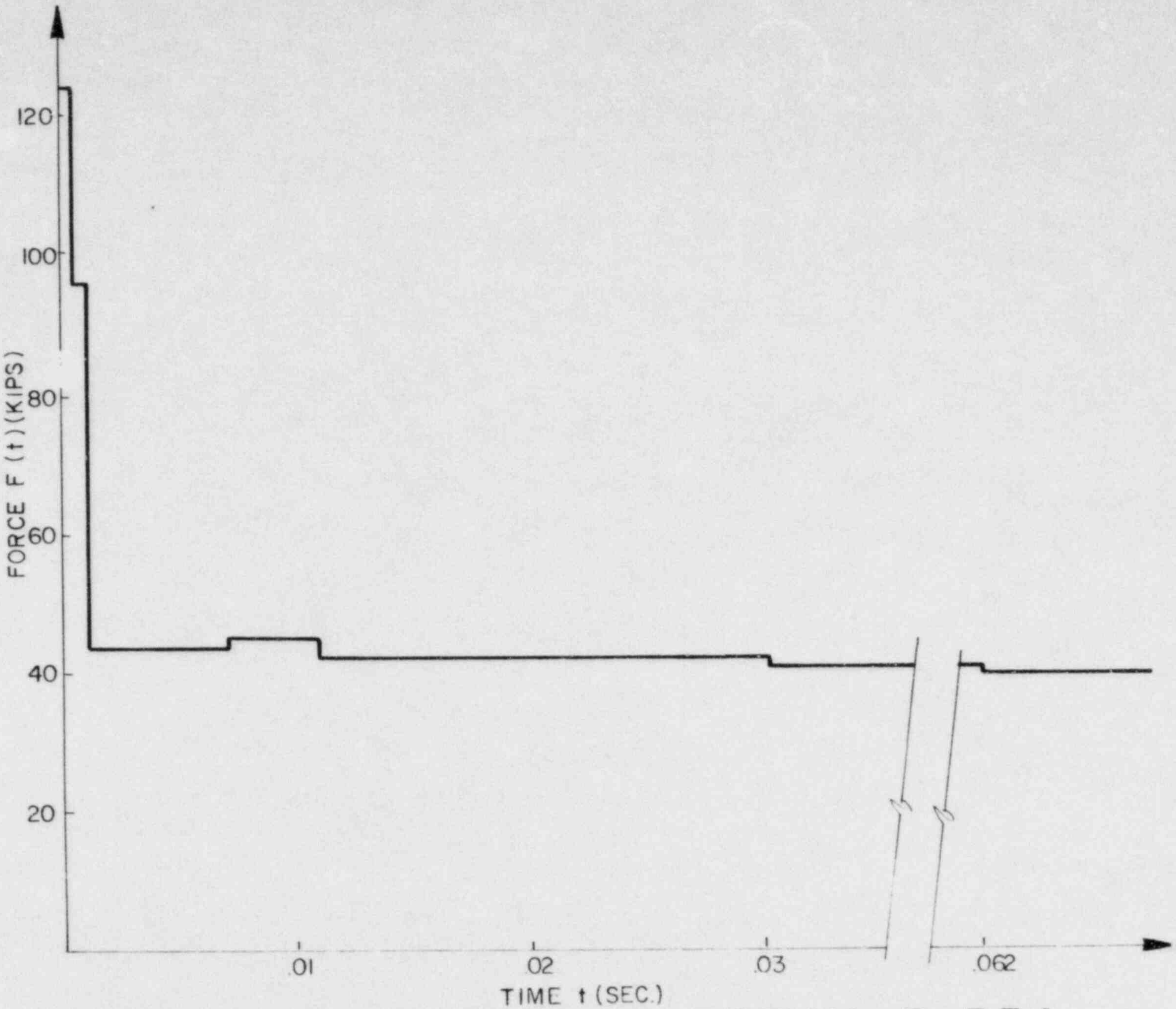

FORCE TIME HISTORY OF BREAK B-55A

FIGURE B4

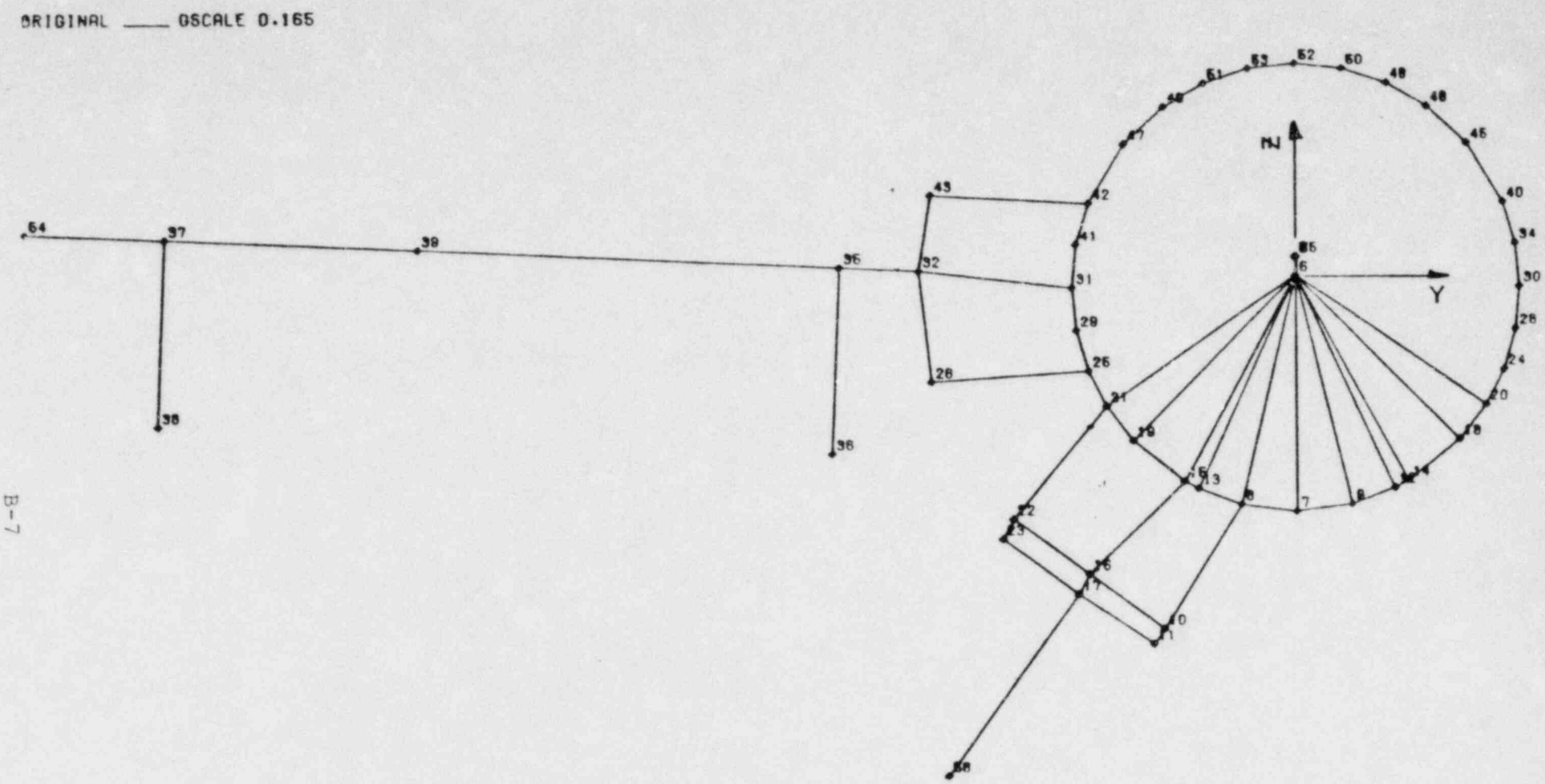

VIEW OF FINITE ELEMENT MODEL IN PLANE OF RESTRAINT FWR-16

FIGURE B5

SAD-442
Rev. 0
September 1984

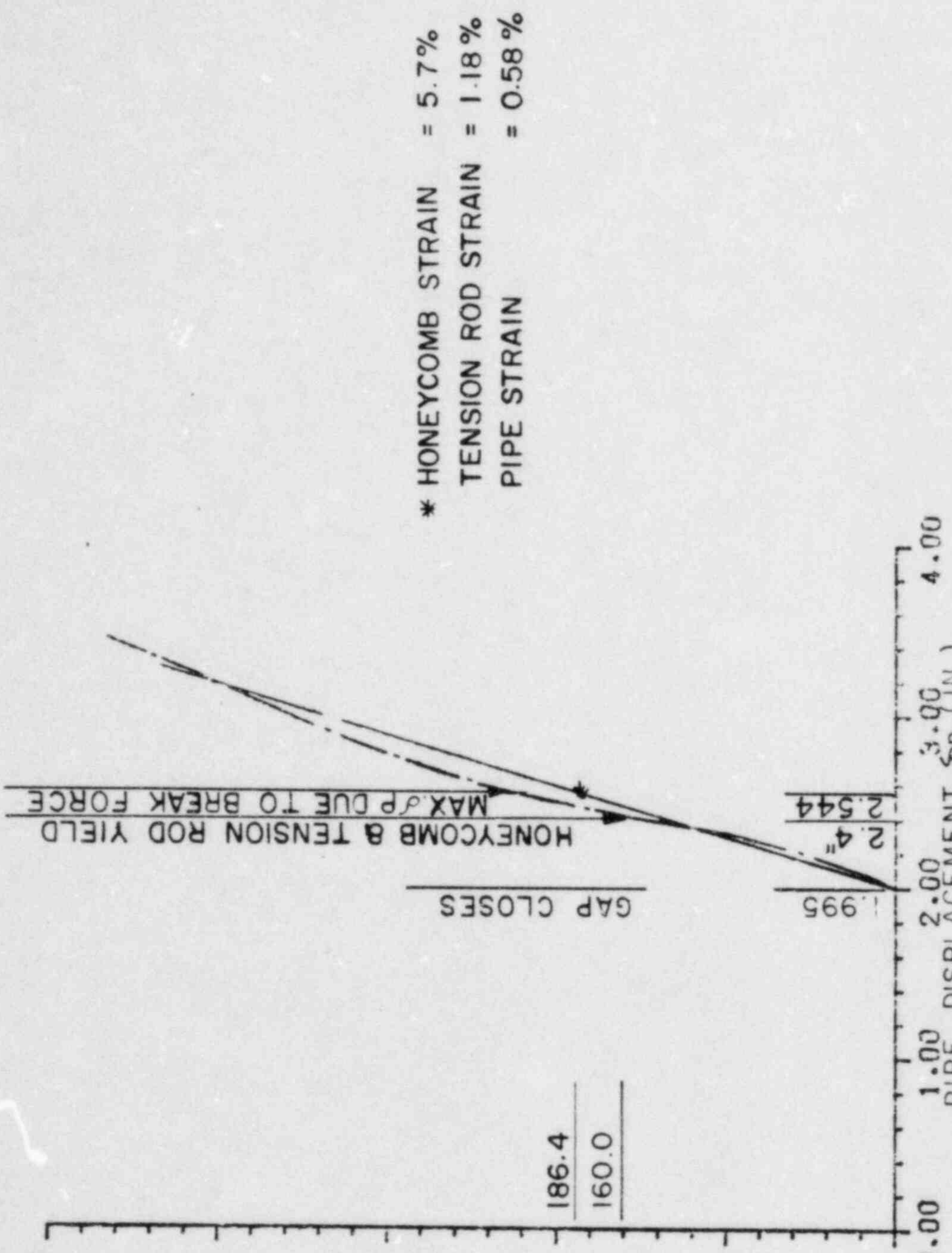

LOAD DEFLECTION CURVE FOR FWR-16

FIGURE B6

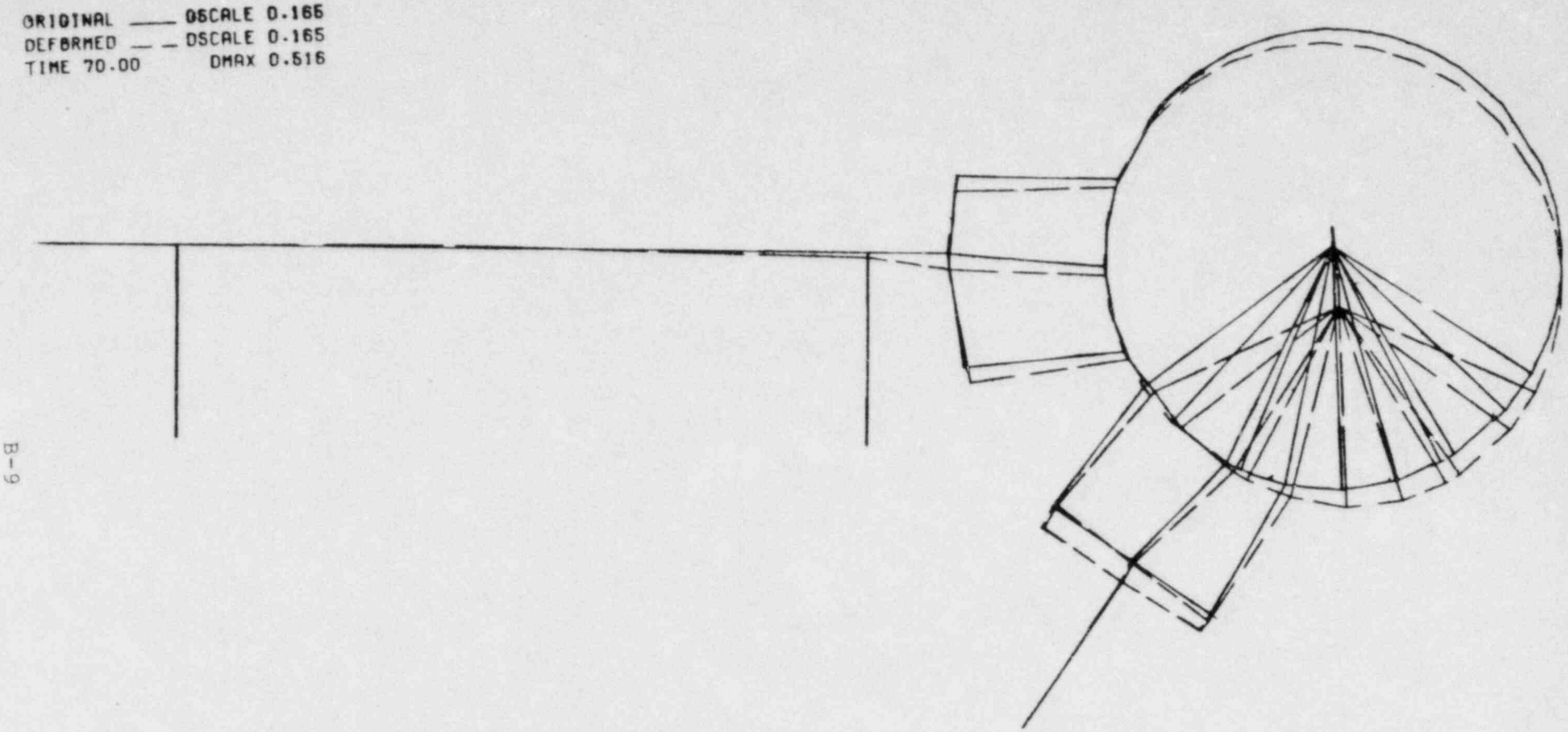

DISPLACED CONFIGURATION OF RESTRAINT FWR-16 AT $\delta_p = 3.12$ IN.

FIGURE B7

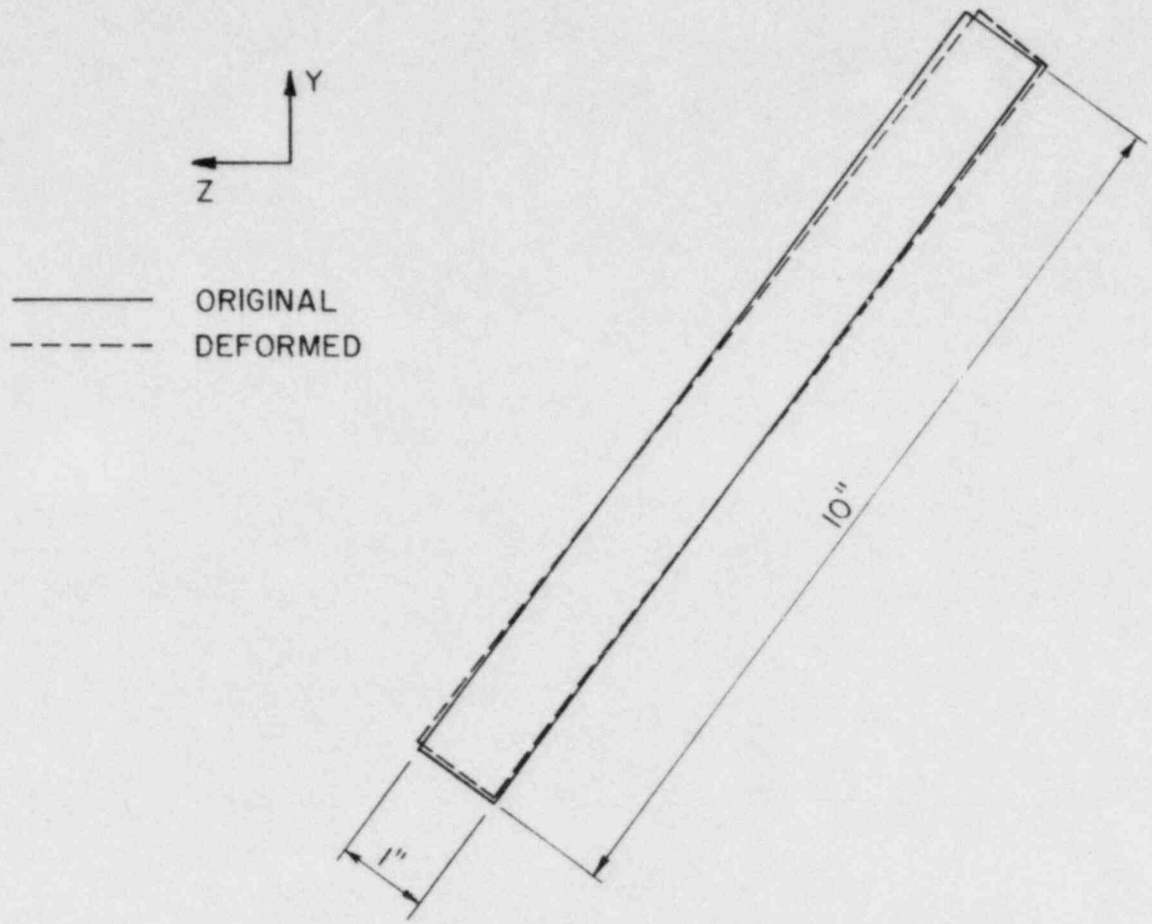

DISPLACED CONFIGURATION OF EAM FOR FWR-16
AT MAXIMUM δp DUE TO PIPE BREAK

FIGURE B8